PROCEEDINGS OF SCIENCE

Challenges in W mass measurements with ATLAS and CMS

Nenad Vranjes[*†]
Institute of Physics, Belgrade, Serbia
E-mail: nenad.vranjes@cern.ch

The mass of the W boson is an important parameter of the Standard Model of particle physics. In this proceedings experimental and theoretical challenges that need to be faced in order to achieve precision of the order of 10 MeV are discussed. The status of various experimental studies related to this measurement are presented.

Fourth Annual Large Hadron Collider Physics
13-18 June 2016
Lund, Sweden

[*]Speaker.
[†]on behalf of the ATLAS and CMS collaborations

PoS(LHCP2016)053

1. Introduction

The Standard Model (SM) [1, 2, 3] with radiative corrections [4] provides a predictive theoretical framework in which the fundamental parameters (particle masses and couplings) are interconnected via an overconstrained set of relations. At lowest order, the W boson mass, m_W, can be written as a function of the Z boson mass, m_Z, the fine-structure constant, α, and the Fermi constant, G_F. Higher order corrections introduce additional dependence of m_W on the gauge couplings and the masses of the heavy particles of the SM. The relation between the parameters is the following:

$$m_W^2\left(1-\frac{m_W^2}{m_Z^2}\right)=\frac{\pi\alpha}{\sqrt{2}G_F}(1+\Delta r), \tag{1.1}$$

where Δr incorporates the effect of higher-order corrections [5, 6]. The Δr term depends strongly on the top and bottom quark masses, m_t and m_b, and logarithmically on the mass of the Higgs boson, m_H. In Beyond standard model (BSM) theories, Δr also receives contributions from additional particles, and the comparison of the measured and predicted values of m_W allows to probe for BSM physics. In the context of global fits of the SM parameters, constraints on BSM physics are currently dominated by the experimental uncertainty on the W boson mass [7].

Previous measurements of m_W were performed at the SPS collider with the UA1 and UA2 experiments [8, 9], at the LEP collider by the ALEPH, DELPHI, L3, and OPAL experiments [10], and at the Tevatron collider by the CDF and D0 experiments [11, 12, 13]. The current world average value of $m_W = 80385 \pm 15$ MeV [14] is dominated by the CDF and D0 measurements performed with $p\bar{p}$ collision data collected and a center-of -mass energy of $\sqrt{s} = 1.96$ TeV [15, 16, 17]. For these results only about 20% (50%) of the total data collected by CDF (D0) is used.

Given the precisely measured values of α, G_F and m_Z, and taking $m_t = 173.34 \pm 0.76$ GeV [18] and $m_H = 125.09 \pm 0.24$ GeV [19] as inputs, the SM prediction of m_W leads to the uncertainty of $\delta m_W = 8$ MeV. The latest most precise measurement of m_t with uncertainty of 0.66 GeV [20] pushes δm_W further to 6 MeV which represents a target for the accuracy of present and future measurements of the W boson mass. Therefore improving the accuracy of the experimental measurements of m_W is of prime importance for testing the overall consistency of the SM. Both Large Hadron Collider (LHC) general purpose experiments, ATLAS [21] and CMS [22], are pursuing the efforts that would lead to the m_W measurement with best possible precision. The ultimate combined precision at the LHC is estimated to be $\delta m_W = 5$ MeV [23].

2. Measurement of m_W at hadron colliders

At hadron colliders, m_W is measured using leptonic decays of the W boson: $W \to \ell\nu$, $\ell = e, \mu$. These represent clean final states with best possible experimental control (in terms of experimental uncertainties). Due to the presence of the neutrino in the final state, m_W is extracted from the kinematic variables measured in the plane perpendicular to the beam direction. Sensitive observables are the transverse momentum of the charged lepton, p_T^ℓ, the transverse momentum of the neutrino, p_T^ν, and the transverse mass of the W boson, $m_T^W = \sqrt{2p_T^\ell p_T^\nu(1-\cos\varphi)}$, where φ is the opening angle between the charged lepton and neutrino momenta in the plane transverse to the

beam. The magnitude and direction of p_T^{ν} are inferred from the missing transverse momentum vector, E_T^{miss}, which corresponds to the momentum imbalance in the transverse plane and defined as $\overrightarrow{E_T}^{miss} = -(\overrightarrow{p_T}^{\ell} + \overrightarrow{u})$. Here u is referred to as the hadronic recoil and corresponds to the measured transverse momentum of the W boson.

The transverse momentum of the charged lepton and the transverse momentum of the neutrino show a Jacobian peak at a value corresponding to $m_W/2$, whereas the transverse mass distribution peaks at the value of m_W. Typically, m_W is determined by comparing the expected final state distributions (templates), predicted with simulated samples for different values of m_W to the measured distribution. Hence the sensitivity to m_W, reflects all the physics aspects of the W boson production and decay processes, as well as the response of the detector. Experimentally, the p_T^{ℓ} and m_T^W distributions are affected by the lepton energy calibration. The m_T^W distribution is also affected by the calibration of the recoil response. The p_T^{ℓ} and m_T^W distributions are broadened by the transverse momentum distribution of the W boson, p_T^W, and are sensitive to the W boson helicity states, which are determined by the proton density functions (PDFs) [24]. Compared to p_T^{ℓ} and m_T, the E_T^{miss} distribution has smaller sensitivity to such physics modeling effects, but larger uncertainties due to the recoil calibration.

With typical selection requirements $30 < p_T^{\ell} < 55$ GeV, $30 < E_T^{miss} < 55$ GeV, $60 < m_T^W < 100$ GeV, $u < 15$ GeV [25], order of several 10^7 $W \to \ell\nu$ candidates are collected per experiment during the LHC Run-1. The available statistics leads to the statistical precision of m_W of O(2 MeV) per experiment, which sets the target scale for the systematic uncertainties. Beside W events, order of 10 milion of $Z \to \ell\ell$ events is collected, which can be used to constrained experimental as well as uncertainties arising from the production and decay of the W boson.

3. Constraining experimental uncertainties

The first major goal in constraining experimental uncertainties is the calibration of the electron energy and muon momentum. The analysed final states of W and Z bosons are dominated by the leptons, the rest of the event consisting of mostly soft hadronic activity. This hadronic activity is considered as a global quantity recoiling against the decaying boson.

After the completion of the Run 1, the LHC experiments have finalised their calibrations and published an extensive set of results on electron, muon and recoil performance [26, 27, 28]. Due to to the large statistics of the collected calibration samples, notably events from low-mass resonances (J/ψ, Υ), as well as leptonic W and Z events, the quality of the modeling of the data by the simulation has been vastly improved compared to the initial performance. However further improvements are desirable for the m_W measurements. For example, the improved muon calibration is derived using the J/ψ and $\Upsilon(1S)$ dimuon decays at CMS for the exercise of an m_Z measurement in the $W-like$ $Z \to \mu\mu$ events [25] , which will be described later. Since the momentum range of the J/ψ and Υ samples is very different from the W and Z ones, the challenge is to find a physically motivated model that describes the detector well in the whole range where the muon momentum measurement precision is dominated by the inner tracker measurement. Three effects are accounted for in the muon momentum calibration to correct the curvature of the muon ($k = 1/p_T$): (i) small variations of the magnetic field, (ii) residual misalignment effects, (iii) imperfect modeling of the material resulting in different energy loss. The magnetic field is a multiplicative factor to the cur-

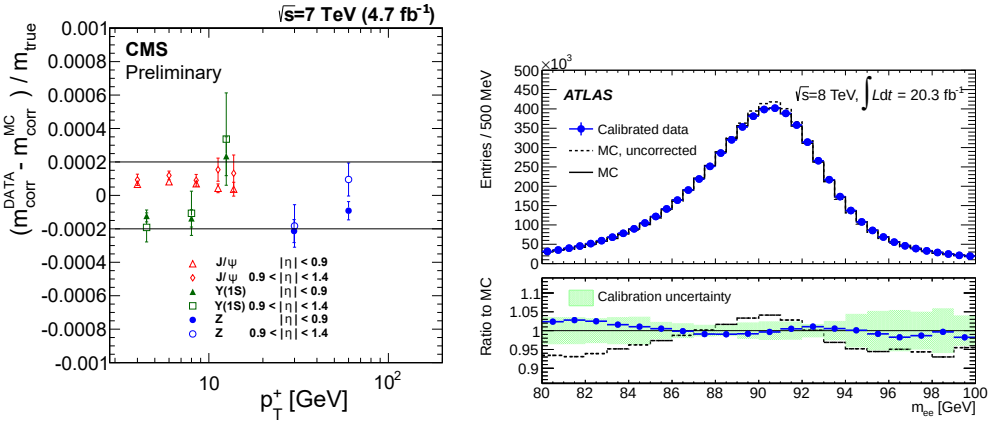

Figure 1: Left: Closure of the calibration of the relative scale (data with respect to MC) for J/ψ, $\Upsilon(1S)$, and Z dimuons, as a function of p_T of the positive muon, after applying the calibration corrections measured with the J/ψ and $\Upsilon(1S)$samples, [25]. Right: Electron pair invariant mass distribution for $Z \to ee$ decays in data and improved simulation. Energy scale corrections are applied to the data. The improved simulation is shown before and after energy resolution corrections, [28].

vature (A) while the misalignment is an additive factor (M) with opposite sign for opposite muon charge. The energy loss correction is an additive term (ε) to the muon momentum (p) resulting in a term that includes angular dependence. The corrected curvature, k^c, is given with:

$$k^c = (A-1)k + qM + \frac{k}{1+k\varepsilon sin\theta}, \tag{3.1}$$

where θ and q are the polar angle and the charge of the muon. The calibration is implemented using a Kalman filter, and its event-by-event uncertainty is estimated by propagating the uncertainties of the two tracks using their full covariance matrices. Corrections are derived for both data and simulation, with values that are found to be typically small: A differs from unity by less than 0.0005, M is less than 10^{-4} GeV^{-1}, and ε is of the order of 4 MeV. The muon momentum resolution is also corrected for. To estimate the closure of the calibration technique, an independent fit is implemented using the J/ψ, $\Upsilon(1S)$, and Z resonances, to measure the difference between the dimuon mass scales obtained in data and in simulation (Fig. 1). Agreement at the 0.2 per-mil level is achieved for the J/ψ and $\Upsilon(1S)$ and Z events, which is the systematic uncertainty of the method.

In the electron channel, J/ψ events are not collected as efficiently, so the Z sample constitutes the main handle on the EM calorimeter energy scale. In the case of electrons, a major difficulty is to understand the calorimeter intercalibration, and the passive detector material upstream of it, before the $Z \to e^+e^-$ peak position can reliably be interpreted in terms of the calorimeter energy scale and used as a reference applying to the W production. The electron calibration closure in $Z \to ee$ events is demonstrated in Fig. 1.

The E_T^{miss} is estimated from the lepton momentum and the measured hadronic recoil. In principle, the hadronic recoil directly reflects the hadronic activity balancing the boson p_T. In practice, however, this quantity is also influenced by other effects, such as the underlying event, multiple parton interactions, and pileup collisions. To reach an accurate control of the E_T^{miss} a precise and

reliably-calibrated measurement of the hadronic recoil is needed, with a required precision of half a percent to match δm_W of 10–20 MeV.

For the reconstruction of the hadronic recoil, ATLAS uses a dedicated recoil algorithm exploited in p_T^W measurement [29]. The calculation is based on the sum over calorimeter cells excluding the cells associated to the lepton. Energy of low-p_T particles is removed along the lepton direction is compensated from the measured underlying event. CMS exploits its Particle flow algorithm [30] ('pfMET') with reconstruction and identification of each particle with an optimised combination of all subdetector information. Similar resolution of $u_\parallel$ is obtained between ATLAS and CMS for the given algorithm. In order to improve the performance of the reconstruction of the hadronic recoil for the m_W measurement CMS uses track-based definition ('tkMET'), where recoil is calculated as a vectorial sum of the p_T of a charged hadron with δz <0.1 cm from the primary vertex. While this definition has the drawback of only retaining 40% of the hadronic recoil probed with the more widely used pfMET, it has the advantages of exhibiting a better data-MC agreement and of being essentially insensitive to pileup. More importantly, it provides, in the presence of pileup, the best discriminating power for the transverse mass Jacobian peak (Fig. 2).

In both experiments, recoil calibration is performed exploiting $Z \to \ell\ell$ events, after lepton calibration is applied. In addition, since the decay is fully measured, momentum balance in the transverse plane can be exploited to determine the response and resolution of the hadronic recoil. To effectively study the properties of the hadronic recoil and partially disentangle the hadronic activity recoiling against the boson p_T from the other effects, the recoil vector is projected along the directions parallel ($u_\parallel$) and perpendicular ($u_\perp$) to the boson p_T direction. Here $u_\parallel$ should be proportional to the boson p_T, the proportionality coefficient depending on the E_T^{miss} definition; $u_\perp$ is expected to be distributed around zero. In CMS $u_\parallel$ and $u_\perp$ are modeled empirically by a sum of three Gaussians, whose parameters are polynomial functions of $p_T^{\mu\mu}$. The calibration is performed in rapidity bins, to minimise uncertainty arising from the vector boson modeling. The models obtained from fitting the different (data and simulated) event samples are used to derive corrections that can be used to transform the original recoil values of a source event sample into corrected values matching the distribution of a target event sample (Fig. 2).

4. Modeling of the W boson production and decay

Measurements of m_W at the LHC are affected by significant complexity related to the strong interaction. In particular, at the LHC centre-of-mass energies and in proton-proton collisions, approximately 25% of the inclusive W production rate is induced by at least one second generation quark (s, c) in the initial state. The amount of heavy-quark-initiated production has implications on the p_T^W distribution, and, as a consequence, the measurement of the m_W is sensitive to the strange and charm quark PDFs. In contrast, second generation quarks contribute only to approximately 5% of the overall W boson production rate at the Tevatron. The most relevant proton PDF constraints are obtained from measurements of the inclusive W^+ , W^- and Z inclusive cross section and rapidity distributions. These observables and their ratios allow, together with slightly more complex final states such $W+c$, a full flavour decomposition of the proton PDFs and a mapping of their Bjorken x dependence. When colliding, the initial state partons radiate a large number of mostly soft gluons, as a result of their mutual interactions. This initial state "parton shower" contributes to

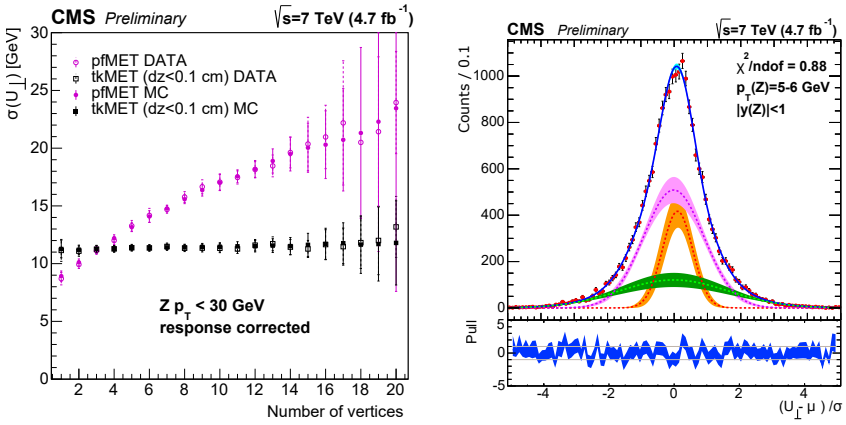

Figure 2: Left: Recoil resolution from Z events as a function of the number of vertices for pfMET (circles) and tkMET (squares), after response correction, from simulated and data samples. Right: Example of the fit to calibration data events using the sum of three Gaussians to the $u_{\parallel}$ distribution, [25].

the transverse momentum distribution of the W and Z. The details of these processes are not fully predictable and are modelled in a semi-phenomenological way tuned via $Z \to \ell\ell$ events. The LHC experiments perform an extensive measurement program that aims at constraining the QCD parameters describing these effects. Strong experimental constraints on the PDFs come from the W cross sections, measured differentially in lepton η. In particular the η-dependent W charge asymmetry is specifically sensitive to the u and d quark valence ratio. These measurements have been pursued by ATLAS and CMS [31]. Z cross section measurements are also performed [32, 33]. In conjunction with the W cross section, this provides information on the strange density [34]. The strange density can also be probed directly, via measurements of $W + c$ production [35]. The non-perturbative parameters are most accurately probed through measurements of the Z boson transverse momentum measurements [36], or of the angular correlations of its decay products [37, 38]. Some results are demonstrated in Fig. 3. The measurements of the correlation of the angular distributions with the lepton transverse momentum distributions, are an important ingredient in m_W measurement. Alternatively constraining p_T^W can be achieved by means of the direct measurement of this observable. However, longer dedicated runs with low pileup would be needed.

Another important aspect for the measurement of m_W is the theoretical description of electroweak corrections, and in particular the modeling of photon radiation from the W and Z boson decay leptons.

5. Z boson mass measurement in $W-like$ events

This analysis performed by CMS [25] consist of a measurement of the Z boson mass using a sample of so-called $W-like$ events, i.e. $Z \to \mu\mu$ events where one of the two muons is removed to mimic the $W \to \mu\nu$ event topology. The analysis is based on the 7 TeV pp data sample collected in 2011, using a single-muon trigger. The sample already provides statistical uncertainties similar to those of the Tevatron m_W results. This exercise represents a proof of principle, showing that the

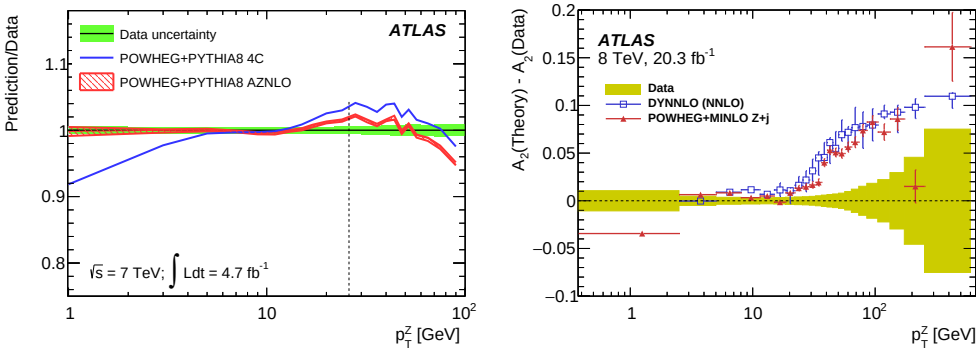

Figure 3: Left: Comparison of tuned predictions to the p_T^Z differential cross sections, for dressed kinematics and in the full rapidity range. Comparison of the POWHEG+PYTHIA8 set-up with the 4C and AZNLO tunes to the same data. The vertical dashed lines show the upper limit of the tuning range [36]. Right: Distributions of the angular coefficients $A2$ as a function of p_T^Z [38].

analysis procedure is reliable and thereby validating the tools and techniques that will be applied in the W boson mass measurement. The Z boson leptonic decays can be triggered and selected at the LHC with high purity. They are used for calibration purposes and their differential cross sections provide precise information about PDFs and the production processes. The transverse momentum distribution of the Z boson can be accurately measured and used to tune non-perturbative parameters in the Monte Carlo generators.

The signal samples are generated with POWHEG [39, 40, 41, 42] linked to PYTHIA8 [43] with tune 4C, interfaced with NLO PDF set NNPDF 2.3 [44]. As this setup does not describe well the boson transverse momentum, p_T^Z is reweighted to data, in bins of 0.5 GeV, to the measured distribution in Z data events. In addition, the default settings of the POWHEG program show discrepancies when compared to the measured angular coefficients of Drell-Yan events, so the $\cos\theta^*$ defined in the Collins-Soper frame is reweighted to data, as a function of the Z rapidity. Since the boson p_T and angular coefficient reweightings are performed in the final fit phase space at reconstruction level, no systematic uncertainty is assigned.

The selected events are required to pass the single trigger requirement and the two muons must have opposite sign with the invariant mass above 50 GeV. The selection of Z events requires both muons to be of high quality, isolated, and have a distance of closest approach between the muon and the beam line $d_{xy} < 0.2$ cm. An event enters in the positive (negative) $W-like$ sample if the $\mu^+(\mu^-)$ is matched to the trigger and fulfills the acceptance conditions $|\eta| < 0.9$, $p_T^\mu > 30$ GeV, while the $\mu^-(\mu^+)$ is only required to have $p_T^\mu > 10$ GeV and $|\eta| < 2.1$. In view of measuring the mass, the analysis only uses the transverse recoil of the boson and the Z transverse component of the muon momentum. A narrow kinematic region, defined to mimic the phase space expected to be selected in the W mass analysis, selects the final sample of $W-like$ events: $30 < p_T^\mu < 55$ GeV, $30 < E_T^{miss} < 55$ GeV, $60 < m_T < 100$ GeV, $u < 15$ GeV, $p_T^{\mu\mu} < 30$ GeV. The background contamination is at the per-mil level, evaluated from MC simulation.

The fits of the sensitive observables are performed in the ranges 32–45 GeV (lepton p_T and E_T^{miss}) and 65–100 GeV (m_T), scaled by the ratio of m_Z^{PDG}/m_W^{PDG} =1.134 to retain a phase space

similar to that intended for the W mass fits. All the fits involving mass measurements are performed with a binned-template likelihood-ratio fitting procedure. Three distributions are independently fitted fixing the normalization of the sum to the number of data events. The statistical correlation has been estimated confirming that m_T^W is highly correlated with both p_T^ℓ and E_T^{miss}, while lepton p_T and E_T^{miss} are practically uncorrelated.

The systematic uncertainty associated with the modeling of the muon efficiencies is evaluated assuming uncorrelated bin-by-bin statistical uncertainties and 1% systematic uncertainties of the "Tag and Probe" methodology. Two sources of systematic uncertainties are considered for the calibration of the lepton momentum scale and resolution: the deviation from perfect closure, and the statistical uncertainty of the calibration sample. Two sources of systematic uncertainties for the mass fits dominated the recoil corrections as well: propagation of the statistical uncertainty of the recoil fits due to the limited statistical accuracy of the calibration sample, and the deviation from the perfect closure of the calibration fits estimated with an alternative model based on an adaptive kernel probability density function. The associated PDF uncertainties are evaluated with the NNPDF 2.3 at NLO set, through a MC-like approach: all 100 NNPDF are tested members and compute the standard deviation. The systematic uncertainty associated with the QED modeling is evaluated by comparing the templates obtained by reweighting the invariant mass distributions with different configurations at generator level, in the full phase space, after final state radiation. The central choice is POWHEG NLO EW+QCD interfaced to PYTHIA 8 for both QCD and QED showers, while the alternative configuration is obtained by switching off the NLO EW contribution. The expected uncertainties are collected in Table 1, symmetrising the largest value between the $\pm 1\sigma$ variations. The results of the fits to the data are shown in Fig. 4, with experimental uncertainties quoted separately from the others.

	m_Z^{W-like}, μ^+			m_Z^{W-like}, μ^-		
Uncertainty	p_T	E_T^{miss}	m_T	p_T	E_T^{miss}	m_T
Muon efficiency	1	1	1	1	1	1
Muon calibration	14	13	14	12	15	14
Recoil calibration	0	9	13	0	9	14
Total exp.	14	17	19	12	18	19
Alternative data rwgt.	5	4	5	14	11	11
PDF	6	5	5	6	5	5
QED	22	23	24	23	23	24
MC Statistics MC	7	6	8	7	6	8
Total other.	24	25	27	24	25	27
Total syst.	28	30	32	30	32	34
Data stat.	40	36	46	39	35	45
Overal	49	47	56	50	48	57

Table 1: Uncertainties on m_Z in $W-like$ events separated by the muon charge [25]. Results are in MeV.

The systematic uncertainties on the lepton momentum and recoil calibrations reflect the present status of the calibrations and may improve in the future by refining the calibration models. The un-

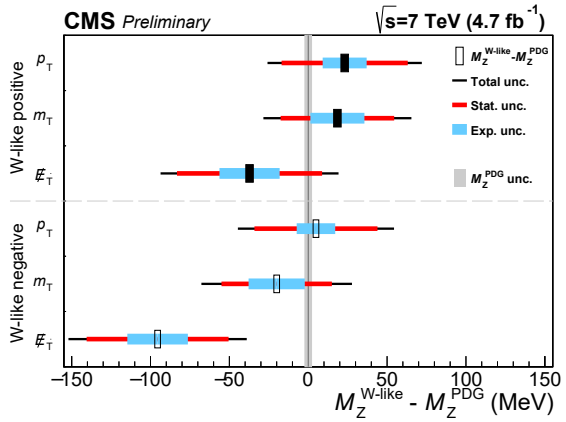

Figure 4: Difference between the fitted mass and Z mass from the PDG, obtained with each of the three observables, together with the corresponding uncertainties [25]. Each of the six measurements can only be considered individually.

certainty related to PDF reflects the knowledge of the parton densities relevant for Z production, that benefits from precise measurements of the p_T^Z and y^Z. This uncertainty will be different and expected to be larger in W events, with the W polarization and charm-initiated processes as the most relevant [24]. On the other hand, when performing the measurement of the W boson mass, the modeling of such aspects will require an extrapolation from the measurements with the Z boson to the expectations for the W boson. The major difficulty arises from correlations among PDF, boson p_T and polarization, and the underlying event, which imply correlated systematic uncertainties in the evaluation of the PDF uncertainties, the systematics of the matrix element, the resummed parts of the calculations, and the parton shower model. In this analysis the largest systematic uncertainty arises from the QED modeling, which is evaluated very conservatively switching on and off the NLO EW contributions in POWHEG. For the m_W analysis this uncertainty needs to be refined which is expected to decrease significantly. Background uncertainty, however, will increase due to larger background level (especially of the hard-to-model multijet background) in the W events.

Special care will be needed for all the systematic constrains performed on Z events when ported to the W, not only to the modeling uncertainties, but also to the experimental ones. For example, recoil response may show some differences in Z and W events, hence systematics due to the calibration performed solely on the Z needs to be addressed.

6. Summary

In short, the detector calibration is at the level required for a first competitive measurement of the m_W at the LHC. The physics modeling of the W boson production and decay represents a major challenge. Ancillary measurements help to constrain physics model and analysis strategy to minimise model dependence and tune state of the art MC. A deep understanding of Drell-Yan production at the LHC is crucial.

Author is supported by Serbian Ministry of Education, Science and Technological development project 171004.

References

[1] S. L. Glashow, Nucl. Phys. **22**, 579 (1961).

[2] A. Salam, Conf. Proc. C **680519**, 367 (1968).

[3] S. Weinberg, Phys. Rev. Lett. **19**, 1264 (1967).

[4] D. Y. Bardin, P. Christova, M. Jack, L. Kalinovskaya, A. Olchevski, S. Riemann and T. Riemann, Comput. Phys. Commun. **133**, 229 (2001) [hep-ph/9908433].

[5] M. Awramik, M. Czakon, A. Freitas and G. Weiglein, Phys. Rev. D **69**, 053006 (2004) [hep-ph/0311148].

[6] A. Sirlin, Phys. Rev. D **22**, 971 (1980).

[7] M. Baak *et al.* [Gfitter Group Collaboration], Eur. Phys. J. C **74**, 3046 (2014) [arXiv:1407.3792 [hep-ph]].

[8] G. Arnison *et al.* [UA1 Collaboration], Europhys. Lett. **1**, 327 (1986).

[9] J. Alitti *et al.* [UA2 Collaboration], Phys. Lett. B **276**, 354 (1992).

[10] S. Schael *et al.* [ALEPH and DELPHI and L3 and OPAL and LEP Electroweak Collaborations], Phys. Rept. **532**, 119 (2013) [arXiv:1302.3415 [hep-ex]].

[11] T. Affolder *et al.* [CDF Collaboration], Phys. Rev. D **64**, 052001 (2001) [hep-ex/0007044].

[12] V. M. Abazov *et al.* [D0 Collaboration], Phys. Rev. D **66**, 012001 (2002) [hep-ex/0204014].

[13] V. M. Abazov *et al.* [CDF and D0 Collaborations], Phys. Rev. D **70**, 092008 (2004) [hep-ex/0311039].

[14] K. A. Olive *et al.* [Particle Data Group Collaboration], Chin. Phys. C **38**, 090001 (2014).

[15] T. Aaltonen *et al.* [CDF Collaboration], Phys. Rev. Lett. **108**, 151803 (2012) [arXiv:1203.0275 [hep-ex]].

[16] V. M. Abazov *et al.* [D0 Collaboration], Phys. Rev. Lett. **108**, 151804 (2012) [arXiv:1203.0293 [hep-ex]].

[17] T. A. Aaltonen *et al.* [CDF and D0 Collaborations], Phys. Rev. D **88**, no. 5, 052018 (2013) [arXiv:1307.7627 [hep-ex]].

[18] ATLAS and CDF and CMS and D0 Collaborations, arXiv:1403.4427 [hep-ex].

[19] ATLAS and CMS Collaborations, Phys. Rev. Lett. **114**, 191803 (2015) [arXiv:1503.07589 [hep-ex]].

[20] CMS Collaboration, CMS-PAS-TOP-14-015.

[21] ATLAS Collaboration, JINST **3**, S08003 (2008).

[22] CMS Collaboration, JINST **3**, S08004 (2008).

[23] M. Baak *et al.*, arXiv:1310.6708 [hep-ph].

[24] ATLAS Collaboration, ATL-PHYS-PUB-2014-015.

[25] CMS Collaboration, CMS-PAS-SMP-14-007.

[26] ATLAS Collaboration, Eur. Phys. J. C **74**, no. 11, 3130 (2014) [arXiv:1407.3935 [hep-ex]].

[27] CMS Collaboration, JINST **10**, no. 02, P02006 (2015) [arXiv:1411.0511 [physics.ins-det]].

[28] ATLAS Collaboration, Eur. Phys. J. C **74**, no. 10, 3071 (2014) [arXiv:1407.5063 [hep-ex]].

[29] ATLAS Collaboration, Phys. Rev. D **85**, 012005 (2012) [arXiv:1108.6308 [hep-ex]].

[30] CMS Collaboration, CMS-PAS-PFT-09-001.

[31] CMS Collaboration, Eur. Phys. J. C **76**, no. 8, 469 (2016) [arXiv:1603.01803 [hep-ex]].

[32] CMS Collaboration, Phys. Lett. B **749**, 187 (2015) [arXiv:1504.03511 [hep-ex]].

[33] ATLAS Collaboration, Phys. Rev. D **85**, 072004 (2012) [arXiv:1109.5141 [hep-ex]].

[34] ATLAS Collaboration, Phys. Rev. Lett. **109**, 012001 (2012) [arXiv:1203.4051 [hep-ex]].

[35] CMS Collaboration, JHEP **1402**, 013 (2014) [arXiv:1310.1138 [hep-ex]].

[36] ATLAS Collaboration, JHEP **1409**, 145 (2014) [arXiv:1406.3660 [hep-ex]].

[37] CMS Collaboration, Phys. Lett. B **750**, 154 (2015) [arXiv:1504.03512 [hep-ex]].

[38] ATLAS Collaboration, arXiv:1606.00689 [hep-ex].

[39] P. Nason, JHEP **0411**, 040 (2004) [hep-ph/0409146].

[40] S. Frixione, P. Nason and C. Oleari, JHEP **0711**, 070 (2007) [arXiv:0709.2092 [hep-ph]].

[41] S. Alioli, P. Nason, C. Oleari and E. Re, JHEP **1006**, 043 (2010) [arXiv:1002.2581 [hep-ph]].

[42] L. Barze, G. Montagna, P. Nason, O. Nicrosini, F. Piccinini and A. Vicini, Eur. Phys. J. C **73**, no. 6, 2474 (2013) [arXiv:1302.4606 [hep-ph]].

[43] T. Sjostrand, S. Mrenna and P. Z. Skands, Comput. Phys. Commun. **178**, 852 (2008) [arXiv:0710.3820 [hep-ph]].

[44] R. D. Ball *et al.*, Nucl. Phys. B **867**, 244 (2013) [arXiv:1207.1303 [hep-ph]].